High Wind Upper Ocean Mixing with Explicit Surface Wave Processes

Peter P. Sullivan
National Center for Atmospheric Research
Boulder, CO 80307-3000
Phone:(303) 497-8953 fax:(303) 497-8171 email: pps@ucar.edu

James C. McWilliams
Department of Atmospheric Sciences and
Institute of Geophysics and Planetary Physics, UCLA
Los Angeles, CA 90095-1565
Phone:(310) 206-2829 fax:(310) 206-5219 email: jcm@atmos.ucla.edu

Grant Number: N00014-09-C-0088

LONG-TERM GOALS

The work described here supports the Office of Naval Research Departmental Research Initiative (DRI) for research on the "Impact of Typhoons on the Ocean in the Pacific" (ITOP). One of central themes of the DRI is to better characterize and predict the ocean boundary layer (OBL) and its impact on typhoon (hurricane) evolution. This is one component of developing improved prediction models for the coupled atmosphere-ocean-wave system. Cooling of the sea surface temperature (SST) is a critical coupling variable influencing atmosphere-ocean hurricane dynamics; SST is largely determined by OBL turbulence, surface wave processes, and mixed layer entrainment. Our research goal is to model the strongly forced wind and wave driven upper OBL using turbulence resolving large-eddy simulation (LES) with explicit wave effects, *viz.,* wave-current interactions and breaking waves and examine their impact on ocean mixing during hurricane events.

OBJECTIVES

The specific research objectives for ITOP are: (1) conduct process studies using LES of the OBL with different combinations of time varying large scale forcings and surface wave effects and examining their impact on ocean mixing; (2) evaluate and compare these LES results with predictions obtained using a 1-D column model of the OBL based on the K-Profile Parameterization (KPP); and (3) compare our simulation results with available observations. Inertial resonance, storm residence time, and the larger scale environment are some of the processes to be examined in our simulations.

Report Documentation Page

Form Approved
OMB No. 0704-0188

1. REPORT DATE	2. REPORT TYPE	3. DATES COVERED
30 SEP 2011		**00-00-2011 to 00-00-2011**

4. TITLE AND SUBTITLE	5a. CONTRACT NUMBER
High Wind Upper Ocean Mixing with Explicit Surface Wave Processes	5b. GRANT NUMBER
	5c. PROGRAM ELEMENT NUMBER
6. AUTHOR(S)	5d. PROJECT NUMBER
	5e. TASK NUMBER
	5f. WORK UNIT NUMBER
7. PERFORMING ORGANIZATION NAME(S) AND ADDRESS(ES) **National Center for Atmospheric Research,Boulder,CO,80307-3000**	8. PERFORMING ORGANIZATION REPORT NUMBER
9. SPONSORING/MONITORING AGENCY NAME(S) AND ADDRESS(ES)	10. SPONSOR/MONITOR'S ACRONYM(S)
	11. SPONSOR/MONITOR'S REPORT NUMBER(S)

12. DISTRIBUTION/AVAILABILITY STATEMENT
Approved for public release; distribution unlimited

13. SUPPLEMENTARY NOTES

14. ABSTRACT

15. SUBJECT TERMS

16. SECURITY CLASSIFICATION OF:			17. LIMITATION OF ABSTRACT	18. NUMBER OF PAGES	19a. NAME OF RESPONSIBLE PERSON
a. REPORT **unclassified**	b. ABSTRACT **unclassified**	c. THIS PAGE **unclassified**	**Same as Report (SAR)**	**12**	

APPROACH

In order to examine the dynamics of the upper ocean boundary layer under high wind forcing we developed an LES model of the OBL that accounts for surface wave effects through non-conservative breaking waves and phase-averaged, conservative wave-current interactions which lead to Langmuir circulations (Sullivan *et al.* 2007). The equations for the resolved flow components are the Craik-Leibovich (CL) theory with crucial wave-current coupling through the vortex force. The larger scale forcing (momentum and scalar fluxes) and wave fields are externally imposed in the LES.

WORK COMPLETED

Meetings: We attended a PI meeting in Santa Fe, NM that focused on a first look at the extensive observation datasets collected during the ITOP field campaign conducted in the Fall of 2010.

OBL LES and Coupling to Wavewatch 3: During the past year, we collaborated extensively with Dr. Leonel Romero from Scripps Institute of Oceanography, who helped us initiate a one-way coupling between the wave prediction model NOAA/NCEP Wavewatch 3 and our LES code for the OBL. This coupling, although very idealized, allows us to drive ocean LES with realistic time and space varying wave fields that are generated by hurricane winds. Thus a consistent set of wind and wave fields are input to the LES. Our canonical surface winds and waves are an idealization of Hurricane Frances (Sanford *et al.*, 2011; Zedler 2007). In addition to the standard suite of variables output by Wavewatch 3 (WW3), the wave spectra are further processed to generate fields pertinent to our air-sea interaction research, *viz.,* wave age, turbulent Langmuir number, Stokes drift velocity, wind-wave alignment, and Stokes depth scale. Preliminary results from the WW3 simulations are discussed in the RESULTS section and will be further described in future publications.

The general design of the LES experiments is to pass a hurricane vortex over small LES domains as sketched in Fig. 1. Now, the surface momentum and scalar fluxes and wave fields imposed at the water surface are those generated by WW3 along selected time slices within the storm path. Our process studies examine the impact of inertially rotating wind stress, resonant and anti-resonant forcing, along lines to the right and left of the storm track.

Two LES computational domains with different horizontal extent are used. On the left hand side $X = -60$ km, which has slightly weaker forcing, a small domain $(L_x, L_y, L_z) = (750, 750, -240)$ m was found acceptable. On the right hand side of the storm, $X = 60$ km, the vigorous forcing and inertially rotating wind stress generates a system of large-scale random gravity waves in the hurricane wake. Test runs indicated that these structures were only adequately captured by increasing the horizontal area of the small domain LES by a factor of 4. Thus, a large domain is used on the right hand side with $(L_x, L_y, L_z) = (1500, 1500, -240)$ m. The number of gridpoints in the small domain is $(N_x, N_y, N_z) = (512, 512, 256)$ and is increased to $(1024, 1024, 256)$ in the large domain; thus the horizontal spacing $\triangle x = \triangle y = 1.46$ m in all the computational boxes. In

the vertical direction, we use a stretched vertical grid where the spacing between any neighboring cells is held fixed at the ratio $K = 1.00451$ with the first gridpoint located at $\triangle z_1 = -0.5$ m. Based on these choices, the cell aspect ratio $\triangle x/\triangle z = (2.93, 1.54)$ at $z = (0, -100)$ m. The small and large computational boxes are able to capture small-scale turbulence at early times and larger scales of motion that develop during the rapid deepening of the OBL at the time of maximum winds.

The initial temperature sounding is simply constructed from two linear segments: Over the depth $h_i \leq z \leq 0$, $\theta = 302.4$ K and for $z < h_i$ the temperature decreases at a rate of 0.04 K m^{-1}. This is approximately the variation observed for Hurricane Frances (Sanford *et al.*, 2011). $h_i = -32$ m is the initial OBL depth. The Coriolis parameter is $f = 0.681 \times 10^{-4}$ s^{-1} which corresponds to an inertial period $T = 25.6$ hrs. The simulations are initiated from rest with small random perturbations in the temperature field under the wind and wave forcing from hour 10 of the WW3 simulation. At this time, the wind and wave fields are slowly varying with winds less than 10 m s^{-1}. Next, these external forcings are held constant and the simulations are integrated for 10 physical hours to generate fully developed equilibrium turbulence. The resulting mean currents are $\mathcal{O}(0.05)$ m s^{-1}, and the initial state of these weak currents has minimal impact on the resulting long time ocean response under strong forcing (Crawford *et al.*, 1996, p. 889). The time step $\triangle t$ in the code is dynamically picked to obey a fixed Courant-Fredrichs-Lewy condition. $\triangle t$ varies by an order of magnitude, from $[0.3 - 5]$ s, and more than 300,000 timesteps are needed to cover the 70 physical hours of the simulation. With a storm translation speed of 5.5 m s^{-1} the LES domains are initially located more than 800 km from the storm center shown in Fig. 1. The parallelization of the code is described by Sullivan & Patton (2011).

RESULTS

The $X - t$ Hovmöller contour maps presented in Figs. 2 and 3 illustrate some of the variability in the wind and wave fields induced by our hypothetical storm over the horizontal domain $X = \pm 300$ km for a time period of more than 50 hrs. In this figure, time is referenced to the time of maximum winds t_m. Thus, the X cross section is ahead of the storm for $t - t_m < 0$ and is behind the storm (in the storm wake) for $t - t_m > 0$. Inspection of the contours in Fig. 2 shows that the windspeed $|\mathbf{U}_a|$ is asymmetrical about $X = 0$ km, a consequence of the storm translation speed V_h, with the largest values ~ 50 m s^{-1} on the right hand side of the storm track.

Given the surface winds the primary output of the wave model is the 2D wave height spectrum $F(\varpi, \Phi)$ which varies with radial frequency ϖ and angular position Φ. The wave spectra are further processed to generate the wave-age field (Fig. 2) and Stokes drift velocity (Fig. 3). Wave age is defined as $\mathcal{A} = C_p/|\mathbf{U}_a|$ where C_p is the phase speed of the peak in the wave height spectrum. $\mathcal{A}$ varies widely in space and time across the storm path. Wave age is a broad indicator of wave breaking activity; the breaking activity tends to increase with decreasing wave age, but also depends on wave steepness. Extensive periods of growing waves $\mathcal{A} \sim 0.5$ are observed near the time of maximum winds with the lowest wave age on the right hand side of the storm. For time periods well ahead of the storm center, $\mathcal{A} \sim 1.2$ indicative of near wind-wave equilibrium conditions. At $t - t_m \sim -20$ hrs, the wave age jumps abruptly, $\mathcal{A} > 2$, as fast moving swell propagates rapidly ahead of the storm eye. In the wake of the storm $t - t_m > 0$, the wave-age again

slowly approaches wind-wave equilibrium and at long times $t - t_m > 20$ hrs the wave state again becomes swell dominated. These estimates of wave age in a hurricane are consistent with values deduced from observations of 1D spectra documented by Young (1998) who reports values ranging from [0.5 - 2.0].

A key variable for our LES is the Stokes drift velocity $\mathbf{u}_s$ which appears in the vortex force $\mathbf{u}_s \times \overline{\boldsymbol{\omega}}$ where $\overline{\boldsymbol{\omega}}$ is the resolved vorticity. For a broadband wave spectrum $\mathbf{u}_s$ is obtained by the integration (Kenyon, 1969)

$$\mathbf{u}_s(z) \;=\; 2\int_0^\infty \int_{-\pi}^{\pi} \mathbf{k}\,\varpi\,F(\varpi,\phi)\,e^{2|\mathbf{k}|z}\,d\phi\,d\varpi \tag{1}$$

where $\mathbf{k}$ denotes the horizontal wavenumber vector. The Stokes drift velocity $\mathbf{u_s}$ inherits the complexity of the wave field through (1); it varies with wind speed, spatial position, and time as depicted in Fig. 3. For our particular choice of storm propagation direction, the largest Stokes drift occurs in component $v_s\,\hat{\mathbf{j}}$ on the right hand side of the storm track. The distribution of the wave field is more asymmetrical than the wind field mainly due to the "extended" fetch on the right hand side of a translating hurricane (Young, 2003). As a result, the distribution of v_s is strongly asymmetrical about $X = 0$ km a reflection of the strongest winds and better wind-wave alignment on the storm right hand side. $u_s\,\hat{\mathbf{i}}$ is clearly largest (most negative) in front of the storm center with contours roughly symmetrical about $X = 0$ km.

Past LES of steady aligned wind-wave cases and a limited number of field observations find vertical velocity is a robust signature of Langmuir turbulence. In the Langmuir turbulence regime, coherent Langmuir cells form and these structures can be detected in the instantaneous vertical velocity field and furthermore impact the statistical (average) moments of $\overline{w}$. Figure 4 compares the maximum resolved second order moment $\langle \overline{w}^2 \rangle_{max}$ and the minimum resolved third-order moment $\langle \overline{w}^3 \rangle_{min}$ diagnosed from our simulations with and without wave effects along the tracks $X = \pm 60$ km. These temporally varying moments are obtained by first computing the vertical profiles $\langle \overline{w(z,t)}^2 \rangle$ and $\langle \overline{w(z,t)}^3 \rangle$ at all z for a given t: $\langle\ \rangle$ denotes an $x-y$ spatial average over the LES domain. $\langle \overline{w(t)}^2 \rangle_{max}$ and $\langle \overline{w(t)}^3 \rangle_{min}$ are found by searching for the appropriate maximum or minimum along their respective vertical profiles and are then normalized by the local surface friction velocity $u_*(X,t)$. We note the vertical locations of the maximum and minimum vary with time. These positions are always located in the upper surface layer of the OBL but are found deeper in the water as the winds and waves increase.

The time series shown in Fig. 4 are compelling evidence for Langmuir turbulence in the hurricane driven OBL. The $w-$moments are sensitive to the location within the storm track, depend on the time and space evolving wind and wave fields, and the inclusion of phase averaged wave-current interactions in the LES. Over the lifetime of the simulation with vortex force $\langle \overline{w}^2 \rangle_{max} > 2$ along the track $X = 60$ km. Notice also that during the time period [-5,5] hours, the maximum vertical velocity variance exceeds 2.5 and this level persists in the hurricane wake. u_* varies by about a factor of 7 over the simulation lifetime and thus the dynamic range of $\langle \overline{w}^2 \rangle_{max}$ is broad. Surprisingly, simple scaling by u_* captures much of the variation in $w-$variance. On the left side of the storm track, the maximum $w-$variance at first tracks its counterpart on the right hand side, then gradually decays, reaches a minimum value at the time of maximum winds, and gradually recovers in the hurricane wake. The differences between the variations on

the right and left hand side of the storm are dramatic and can be traced to the wave fields and wind-Stokes alignment. The mis-aligned wind and wave fields and the very low values of Stokes drift around the time of maximum winds on the left hand side of the storm track effectively shut off the vortex force. In the simulations without vortex force, the maximum $w-$variance is nearly independent of the track position and is $\mathcal{O}(1)$, similar to what is expected for a flat-wall boundary layer flow.

The impact of wave-current interactions on the third-order vertical velocity moment is even more impressive upon comparing cases with and without vortex force. With vortex force the minimum third-order moment can be 10 times larger than its no vortex force counterpart. Thus we find CL mechanics are active and critical in our simulations but varies with the wave state. The surface Stokes drift velocity on the right side of the storm track scales reasonably well with the local friction velocity u_*. Our results are in good agreement with the measurements of D'Asaro (2001).

Flow visualization of the instantaneous vertical velocity at the time of maximum winds is compelling evidence for Langmuir turbulence. In Fig. 5, we show images of resolved $\overline{w}/u_*$ from two simulations: the upper panel is from the left (non-resonant) side while the lower panel is from the right (resonant) side of the storm track. As expected based on the time series of $\langle \overline{w}^2 \rangle_{max}$ and $\langle \overline{w}^3 \rangle_{min}$ shown in Fig. 4, there is scant evidence for the formation of Langmuir cells on the left hand side of the track. In contrast, impressive vertically oriented streaks are found on the right hand side. Note at this time the winds and stresses in the lower image are oriented in the positive y direction (see vectors in the image). The streaks show mergers and are found to significantly alter the turbulent dynamics in the upper OBL. Thus, wave-current interactions are most active on the resonant side of the storm.

IMPACT/APPLICATIONS

The LES results obtained here for hurricane driven OBLs can be used to guide the interpretation of observations collected during the ITOP program. In addition, the results can be used to test simpler 1-D parameterizations of the ocean mixed layer that are used in large scale models. Our particular interest is in evaluating and improving the so-called K-profile parameterization (KPP) that is routinely used in the Regional Ocean Modeling System (ROMS).

TRANSITIONS & RELATED PROJECTS

The present work has links to the ONR DRI on High Resolution Air-Sea Interaction (HIRES) that focuses on the interaction of waves and turbulence in the atmospheric surface layer. For a description of HRES see http://airsea.ucsd.edu/hires/. The LES model being developed for HIRES is also being used in the present work.

REFERENCES

D'Asaro, E., 2001: Turbulent vertical kinetic energy in the ocean mixed layer. *Journal of Physical Oceanography*, **31**, 3530-3537.

Grant, A. L. M. & S. E. Belcher, 2009: Characteristics of Langmuir turbulence in the ocean mixed layer. *Journal of Physical Oceanography*, **39**, 1871-1887.

Kenyon, K. E., 1969: Stokes drift for random gravity waves. *Journal of Geophysical Research*, **74**, 6991-6994.

McWilliams, J.C., P. P. Sullivan & C-H. Moeng, 1997: Langmuir turbulence in the ocean. *Journal of Fluid Mechanics*,**334**, 1-30.

Sanford, T. B., J. F. Price & J. B. Girton, 2007: Highly resolved observations and simulations of the ocean response to a hurricane. *Journal of Physical Oceanography*, **41**, 1041-1056.

Sullivan, P.P., J.C. McWilliams, & W.K. Melville, 2007: Surface gravity wave effects in the oceanic boundary layer: Large-eddy simulation with vortex force and stochastic breakers. *Journal of Fluid Mechanics*, **593**, 405-452.

Sullivan, P. P. & E. G. Patton, 2011: The effect of mesh resolution on convective boundary layer statistics and structures generated by large-eddy simulation. *Journal of the Atmospheric Sciences*, [in press].

Tseng, R-S. & E. D'Asaro, 2004: Measurements of turbulent vertical kinetic energy in the ocean mixed layer from Lagrangian floats, *Journal of Physical Oceanography*, **34**, 1984-1990.

Young, I. R., 1998: Observations of the spectra of hurricane generated waves. *Ocean Engineering*, **25**, number 4-5, 261-276.

Young, I. R., 2003: A review of the sea state generated by hurricanes. *Marine Structures*, **16**, 201-218.

Zedler, S.E, 2007: *Strong wind forcing of the ocean.* PhD Thesis, University of California, San Diego, San Diego, California, pp. 127.

PUBLICATIONS

Sullivan, P. P. & E. G. Patton, 2011: The effect of mesh resolution on convective boundary layer statistics and structures generated by large-eddy simulation. *Journal of the Atmospheric Sciences*, [in press].

Weil, J. C., P.P. Sullivan, E. G. Patton & C-H. Moeng, 2011: Statistical variability of dispersion in the convective boundary layer: LPDM-LES model ensembles and observations. *Boundary-Layer Meteorology*, [submitted].

Nilsson, E. O., A. Rutgersson & P. P. Sullivan, 2011: Convective boundary layer structure in the presence of wind-following swell. *Quarterly Journal of the Royal Meteorological Society*, [submitted].

Van Roekle, L. P., B. Fox-Kemper, P. P. Sullivan, P. E. Hamlington & S. R. Haney, 2011: The form and orientation of Langmuir cells for misaligned winds and waves. *Journal of Geophysical Research*, [submitted].

Hanley, K. E., S. E. Belcher & P. P. Sullivan, 2011: Response to "Comments on a global climatology of wind-wave interaction". *Journal of Physical Oceanography*, [in press].

Moeng, C.-H. and P.P. Sullivan 2011: Large Eddy Simulation. Encyclopedia of Atmospheric Sciences 2nd Edition, Eds. G. North, F. Zhang and J. Pyle. Academic Press, [submitted].

Liang, J., J. C. McWilliams, P. P . Sullivan & B. Baschek, 2011: Modeling bubbles and dissolved gases in the ocean. *Journal of Geophysical Research – Oceans*. **116**, C03015, 1-17.

Kukulka, T., A. J. Plueddemann, J. H. Trowbridge, & P. P. Sullivan, 2011: The influence of crosswind tidal currents on Langmuir circulation in a shallow ocean. *Journal of Geophysical Research –Oceans*, **116**, C08005, 1-15.

Lenschow, D. H., M. Lothon, S. D. Mayor, P. P. Sullivan, & G. Canut, 2011: A comparison of higher-order vertical velocity moments in the convective boundary layer from lidar with in situ measurements and LES. *Boundary-Layer Meteorology*, [in press].

Suzuki, N., T. Hara, & P. P. Sullivan, 2011: Turbulent airflow at young sea states with frequent wave breaking events: Large eddy simulation. *Journal of the Atmospheric Sciences*, **68**, 1290-1305.

Patton, E. T. Horst, P. Sullivan, D. Lenschow, S. Oncley, W. Brown, S. Burns, A. Guenther, A. Held, T. Karl, S. Mayor, L. Rizzo, S. Spuler, J. Sun, A. Turnipseed, E. Allwine, S. Edburg, B. Lamb, R. Avissar, R. Calhoun, J. Kleissl, W. Massman, K. Paw-U, & J. Weil, 2011: The canopy horizontal array turbulence study (CHATS). *Bulletin of the American Meteorological Society*, **92**, 593-611.

Moeng, C.-H. Moeng, P. P. Sullivan, M. F. Khairoutdinov, & D. A. Randall, 2010: A mixed scheme for subgrid-scale fluxes in cloud-resolving models. *Journal of the Atmospheric Sciences*, **67**, 3692-3705.

Sullivan, P. P. and E. G. Patton, 2011: Offshore marine boundary-layer winds predicted by a large eddy simulation model with resolved surface waves. *6th Theoretical Fluid Mechanics Conference*, American Institute of Aeronautics and Astronautics, Honolulu, HI.

Nguyen, K. X. S. P. Oncley, T. W. Horst, P. P. Sullivan & C. Tong, 2010: Investigation of subgrid-scale turbulence in the atmospheric surface layer using AHATS field data. *American Physical Society, Fluid Dynamics*, Long Beach, CA.

Suzuki, N., T. Hara, & P. P. Sullivan, 2010: Turbulent airflow at young sea states with frequent wave breaking events: Large eddy simulation. *17th Conference on Air Sea Interaction*, Annapolis, MD.

Liang, J., J. C. McWilliams, P. P . Sullivan, 2010: Modeling gas bubbles in the ocean boundary layer. *17th Conference on Air Sea Interaction*, Annapolis, MD.

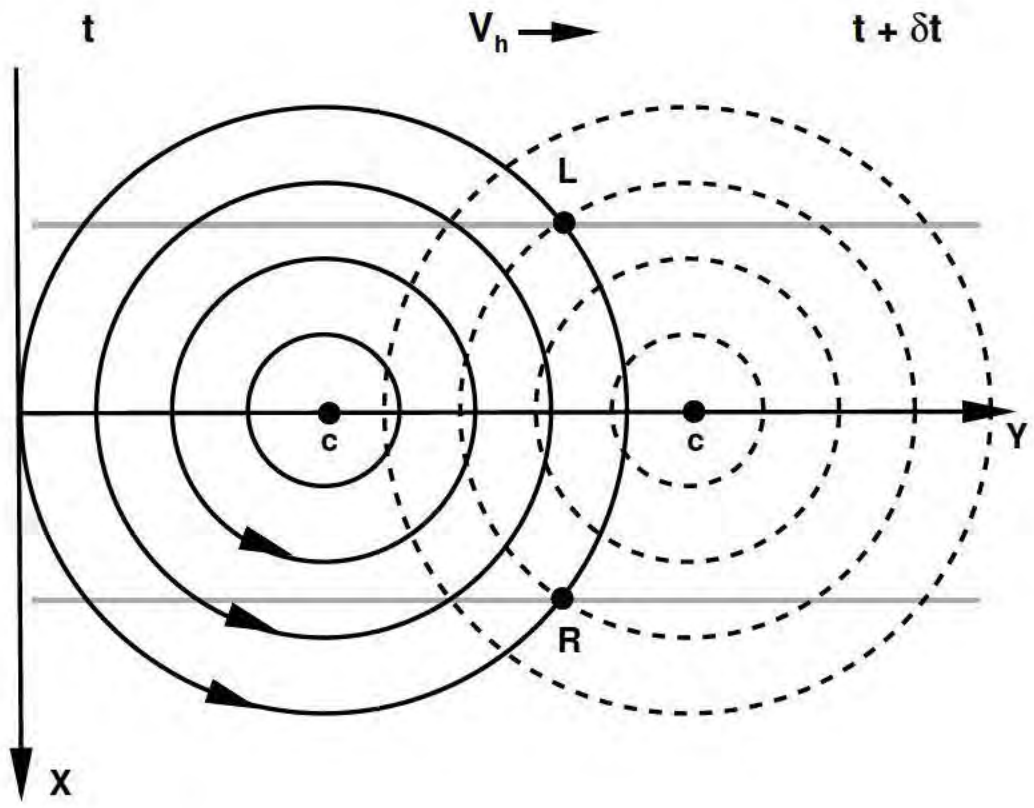

Figure 1: Sketch of an idealized hurricane vortex used for setting the surface forcing conditions in LES. The vortex propagates left to right with speed V_h and has a characteristic length scale (radius of maximum winds) Λ. The families of solid and dotted circles indicate the position of the vortex at initial time t and at a later time $t + \triangle t$, respectively. The fixed points (R, L) to the right ($X > 0$) and left ($X < 0$) of the vortex center (c) feel the time history of winds and waves along the horizontal gray lines.

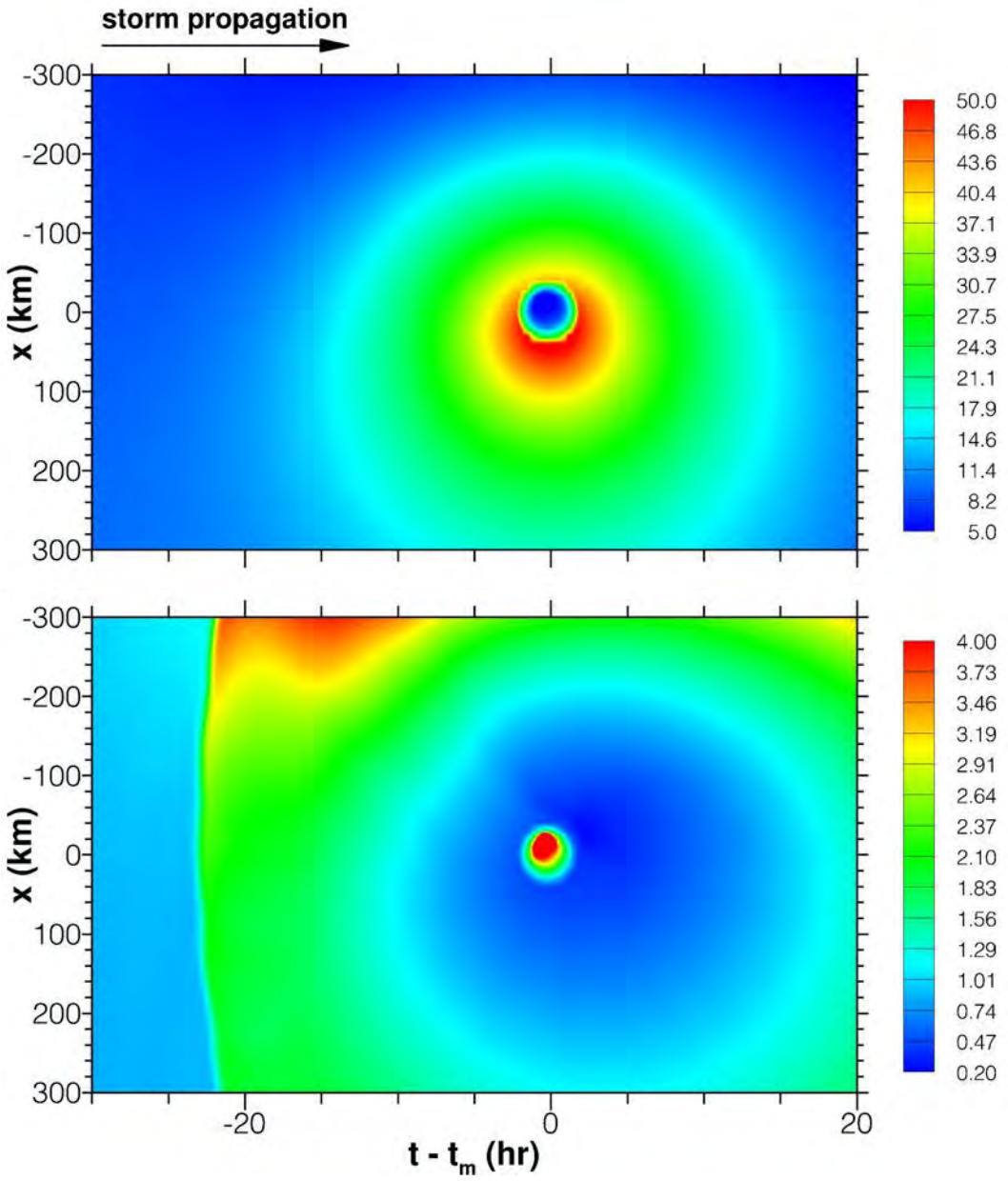

Figure 2: *The hurricane vortex propagates left to right and the fields are shown in the form of an X-t Hovmöller diagram, i.e., the temporal variation of a particular field is shown for a chosen x cross section. Time is referenced to the time of maximum winds t_m. The upper panel shows contours of wind speed (in m s^{-1}) imposed in the Wavewatch 3 simulations. The lower panel depicts the wave age $\mathcal{A} = C_p/|\mathbf{U}_a|$ over the lifetime of the storm.*

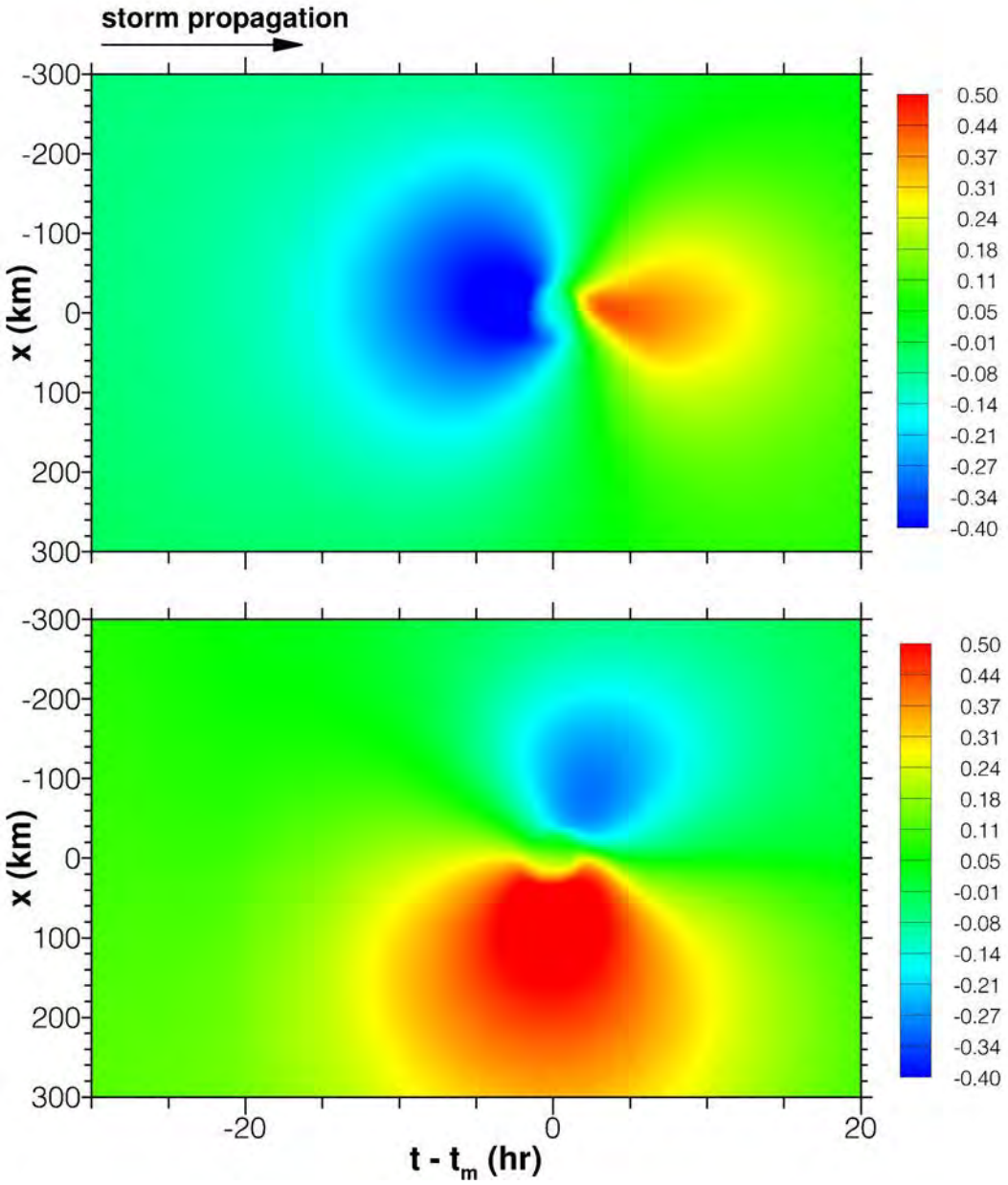

Figure 3: Upper and lower panels show the Stokes velocity components (u_s, v_s) at the water surface for the imposed wind field. The color bar is in units of $\mathrm{m\,s^{-1}}$.

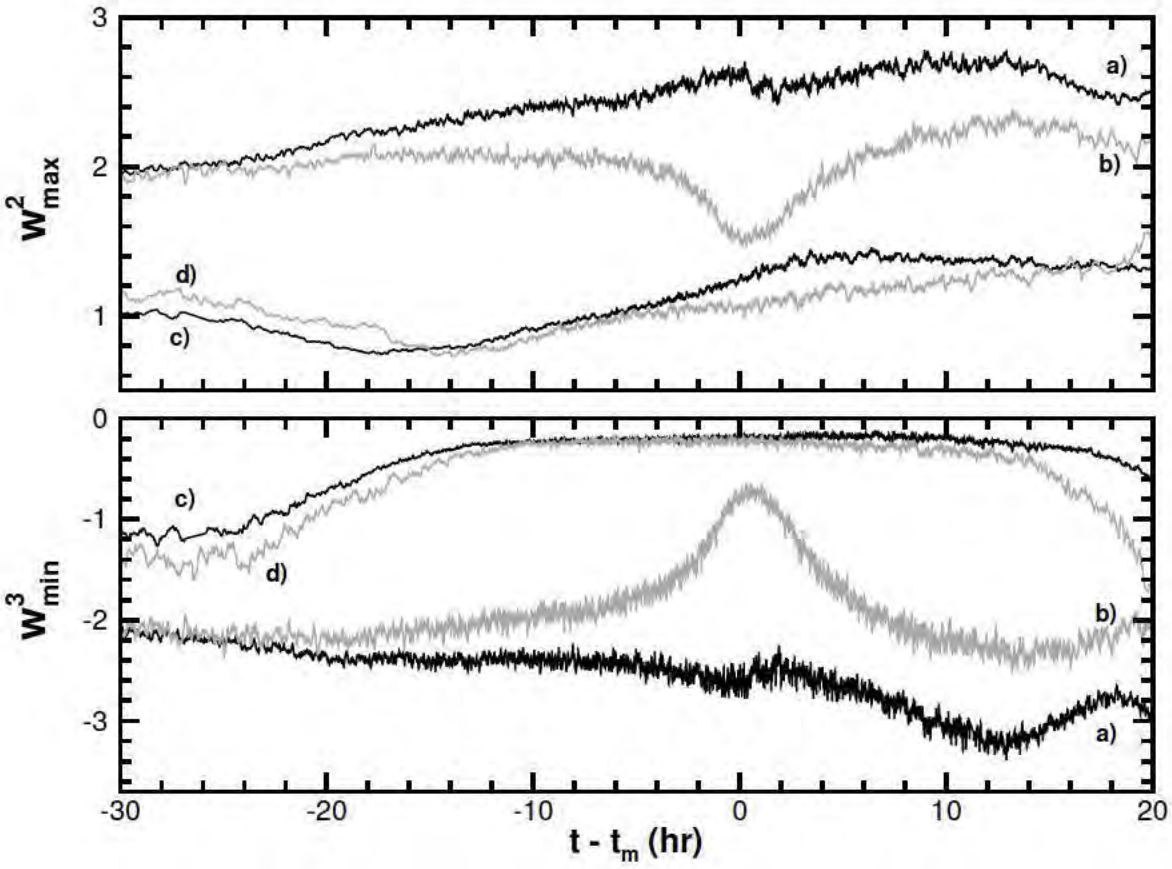

Figure 4: *Temporal variation of the maximum resolved vertical velocity variance* $\langle \overline{w}^2 \rangle_{max}$ *and minimum resolved third-order moment* $\langle \overline{w}^3 \rangle_{min}$ *for cases with and without wave effects and locations left and right of the storm center. Simulations with wave effects [a)* $X = 60$ *km, b)* $X =$ *-60 km] and simulations with no wave effects [c)* $X = 60$ *km, d)* $X =$ *-60 km]. The normalization is by* $u_*(X,t)$.

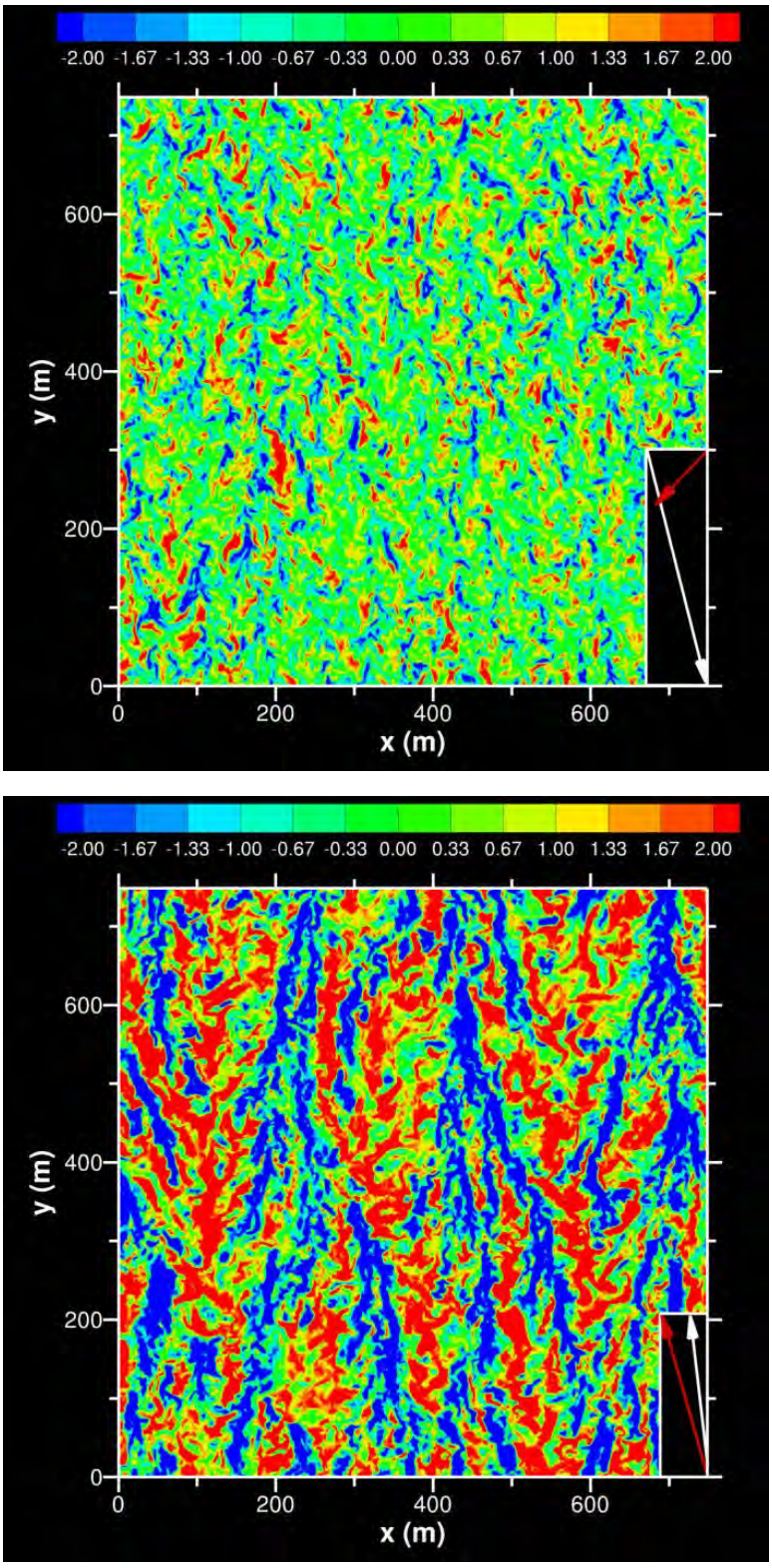

Figure 5: *Flow visualization of the vertical velocity field normalized by local u_* on the left (upper panel) and right (lower panel) sides of the storm at the time of maximum winds. The arrows indicate the direction of the wind (white) and Stokes drift (red). Note the formation of vigorous Langmuir cells on the right hand side of the storm track.*